Fluid Contact Angle Assessment to Evaluate Wetting of Dental Materials

by Rana Abdelsalam, M.S.B.E.

May 2017

Directed by: Teresa Ryan, Ph.D.

Department of Engineering

Dental crowns account for a large percentage of restorative dental procedures, but the crown materials have been shown to cause wear on the natural opposing tooth. There is uncertainty regarding which mechanical or chemical process is the exact cause of wear. The premise of this work is that wear on the natural opposing enamel is due to lack of salivary adherence on the crown material, rather than the surface roughness of crown materials. The purpose of this work is to evaluate the presence of salivary lubrication on dental crown materials by measuring liquid contact angle on different material samples. The following dental crown materials types were evaluated: resin nano-ceramics, leucite-reinforced glass-ceramics, feldspathic porcelain, lithium disilicate glass ceramic, and zirconia. A Ramé-Hart Drop Image goniometer was used for the contact angle measurements along with an image processing software that was developed in MATLAB to complement the goniometer measurements. Statistical analysis was done via JMP software using the Tukey-Kramer method for multiple comparison analysis of the different materials. The results showed that some crown material were more hydrophobic than others, hence adequate wetting of the material did not occur. The resin nano-ceramics material is the most hydrophobic dental crown material with a contact angle of $60.5°$, while zirconia is the most hydrophilic material with a contact angle of $20.4°$. MATLAB angle measurements supported the goniometer measurements. The contact angle measurements obtained from this work correlate with wear studies by a number of authors.

This work provides the first known experimental results to investigate the effect of lubrication on different crown materials.

Fluid Contact Angle Assessment to Evaluate Wetting of Dental Materials

A THESIS

Presented to the Faculty of the Department of Engineering

College of Engineering and Technology

East Carolina University

In Partial Fulfillment of the Requirements For the Degree

Master of Science in Biomedical Engineering

by

Rana Abdelsalam

May, 2017

Fluid Contact Angle Assessment to Evaluate Wetting of Dental Materials

By

Rana Abdelsalam

APPROVED BY:

DIRECTOR OF
THESIS: ————————————————————————————

Teresa Ryan, Ph.D.

COMMITTEE MEMBER: ————————————————————————

Waldemar de Rijk, Ph.D.

COMMITTEE MEMBER: ————————————————————————

John Choi, Ph.D.

CHAIR OF THE
DEPARTMENT OF ENGINEERING: ——————————————————

O. Hayden Griffin, Ph.D.

DEAN OF THE
GRADUATE SCHOOL: ————————————————————————

Paul J. Gemperline, Ph.D.

ACKNOWLEDGMENTS

TABLE OF CONTENTS

LIST OF TABLES

LIST OF FIGURES

CHAPTER 1

INTRODUCTION

1.1 Problem Statement and Proposed Work

The interaction between saliva and anatomical structures within the mouth is pivotal for overall oral health and physiology. Dental crowns act as a protective barrier, cupping and surrounding a tooth, but they have been found to cause degradation on the natural opposing tooth. The idea that drives this project is the assertion that saliva does not adequately adhere to dental crown material surfaces. This lack of adherence leads to the lubrication effect of saliva being lost, causing the crown material to grind on the opposing tooth which leads to degradation and damage to the tooth enamel. Understanding the material interaction with saliva will provide further insight on surface treatment specifications of crown materials. This insight will improve future material development. The purpose of this project is to determine how well saliva lubricates dental crown materials by measuring the contact angle of water and artificial saliva on the material. A Ramé-Hart Drop Image goniometer was used for angle measurements and a custom MATLAB image-processing software was developed to complement goniometer measurements. Measurements of water were used to validate the goniometer by comparing the measured values to literature values. The hypothesis is that crown materials that cause more wear on the natural opposing tooth will have larger contact angle values. A large contact angle indicates that saliva is not wetting the tooth surface, and is therefore not providing the necessary lubrication that prevents degradation. Wear data on specific crown materials will be assessed and compared to contact angle measurements to evaluate correlation. This work is relevant to those interested in studying both the physiological and the material science perspective of dental materials.

1.2   Organization of Thesis

This document is organized as follows. Chapter 2 provides the background information on topics that support this work. Topics in Chapter 2 include the (1) role of saliva in the mouth, (2) contact angles, (3) dental crown material and (4) image processing. Wear data caused by crown materials reported in literature is of central interest to this work. An overview of the existing wear depth data is given in Section 2.3.2. Chapter 3 describes the experimental portion of this work, which involves the goniometer. Specifically, Section 3.1.1 provides a list of the different materials used, Section 3.1.2 explains how the crown materials are prepared, Section 3.1.3 explains the experimental method and the different terminology associated with these methods and the goniometer data analysis approach is presented in Section 3.1.4. All goniometer results are discussed in Section 3.2. Chapter 4 discusses the image processing software that was developed to measure the contact angle and complement the goniometer measurements. Sample images and MATLAB results are presented in Sections 4.2.1 and 4.3. In Chapter 5, correlation of contact angle measurements and literature wear data are discussed. Possible sources of error in this work are presented in Section 5.3. This work is summarized and conclusions are made in Chapter 6. All the different measurements taken throughout the course of this work are presented in the Appendix.

CHAPTER 2

BACKGROUND INFORMATION

In this chapter, background information is provided on different components that play a crucial role in understanding this work are discussed. These components include: the importance of saliva in the mouth, explanation of the contact angle, the role of crown materials in dentistry and the wear data caused by these materials.

2.1 Saliva

2.1.1 Variability

Humans normally secrete about 1-1.5 L of saliva each day. Saliva is composed of mainly water (99.0-99.5%) and of inorganic and organic substances including immunoglobulins, proteins, enzymes, mucins, and nitrogenous products (0.5-1%) [1]. However, saliva does vary from person to person and from day to day [2]. Natural saliva is too variable and inconsistent in nature for use in a controlled study application. Duplicating the exact properties of human saliva in a research project is not practical and will add unnecessary lurking variables and sources of error. Thus, the use of artificial saliva was deemed more appropriate for this work.

2.1.2 Physiological Function

Saliva plays a pivotal role in the mouth by providing digestive and protective functions. Saliva aids in the remineralization process of teeth by supplying calcium and phosphate to the enamel. It acts as an acid neutralizer by releasing bicarbonate in the mouth to regulate the pH during eating and drinking [3]. When the pH increases, remineralization of softened tissue does not occur, which

leads to dental erosion. Dental erosion is defined as the progressive loss of dental tissue and tooth structures that is caused by chemical processes occurring in the mouth [4]. The pH regulation from saliva also lessens the severity of dental erosion.

Saliva forms a protective film on all surface in the mouth. When saliva adheres to a material, the salivary film is created. Salivary proteins are found on the adsorbed film and allow saliva to provide its digestive and protective functions, such as lubricating the oral cavity and helping with food digestion. The adsorption of saliva on different surfaces of the mouth is a selective process. The dental material upon which the salivary film adsorbs influences the film formation in the mouth [2]. Without proper film formation, dry mouth and degradation of teeth are possible outcomes. In addition to its biochemical role described above, saliva has a biomechanical role as well. It acts as a lubricant by providing lubricatory molecules that coat the oral soft tissue, which minimizes the friction between two surfaces in the mouth [5].

2.1.3 Lubrication

The adsorbance and lubrication of saliva on a surface helps with speech, swallowing of food, and protecting oral surfaces from abrasion, wear, and plaque adhesion. According to Reeh et al, salivary lubrication is one of the factors that helps minimize and control the occlusal or surface wear of natural teeth [6]. The salivary film formed on the surface of the teeth prevents opposing teeth from grinding against one another during normal daily activities such as speech and chewing.

In engineering science, the effect of a liquid that is trapped in between two surfaces in contact is referred to as the secondary lubrication. The liquid can be squeezed by the relative movement of those surfaces to reduce friction [7]. Saliva is providing a secondary lubrication effect in the mouth when it is trapped between two opposing tooth surfaces or between a restoration and tooth surface. Ma *et al.* sought to evaluate the lubrication effect on the performance of hip joint replacements. This work found that the presence of lubricants strongly affects the wear mechanism and wear rate of the device in the body: the greater the lubrication, the lower the wear rate of the hip replacement

device in the body [8]. The effect of lubrication between a crown and an opposing tooth surface can be compared to the lubrication seen in such implants. The presence of the saliva provides lubrication between the crown surfaces and opposing teeth.

The interaction between the lubricant and solid interfaces determines the strength of lubrication, and is characterized by molecular adhesion. The contact angle of a liquid on a solid surface is related to the intermolecular attractive forces, or the molecular adhesion between the lubricant and the solid interface [9, 10]. This project will use contact angle measurements as a way to assess the relative amount of lubrication of saliva on various material surfaces.

2.2 Contact Angles

In this study, the lubrication effect of saliva is evaluated by measuring the contact angle of artificial saliva and water on various materials. The contact angle is the measurable angle of a small drop of liquid that forms on a solid surface [11]. It also measures how well a liquid can wet and adhere to a surface. Measurement of the contact angle is used to determine the solid-liquid and vapor-solid interfacial tensions present in the materials, which shows the bonding relationship between two surfaces [12]. Studies have used the contact angle method to determine the lubrication effect of a lubricant on a solid interface [9, 13]. The contact angle is also used as a traditional method for determining hydrophilicity of a material. Lower contact angles indicate increased wettability or greater hydrophilicity, while greater contact angles indicate limited wettability or greater hydrophobicity. A large contact angle also indicates weak adhesive forces between the liquid and the solid [9].

Contact angle measurements may be affected by experimental conditions such as drop volume, temperature, and surface impurities. The drop size used affects the contact angle value [14]. Contact angle measurements varies by $5°$ as the radius of the drop size varies from 1 to 5 mm [15, 16]. Kugel et. al. evaluated the effect of drop size variation on contact angle. That work found that

variations resulted in different contact angle values, but not significant enough to result in a dramatic change in the ranking of the hydrophilic behavior of the materials [17]. Surface impurities such as heterogeneity and roughness of the material can impact the point of contact and cause variations in contact angle measurements [18]. Despite the variations that can be caused due to drop volume and surface impurities, the contact angle method yields an accuracy of approximately $2°$ [15]. According to Karmouch *et al.*, contact angle measurements are affected by surface temperatures that are below $5°C$ [19]. Bernardin *et al.* found that temperatures above $120°C$ also affected contact angle measurements [20]. Palamara *et al.* conducted an experiment on contact angles of CO_2 brine quartz systems and found that the contact angle changes by $0.18°$ for every $1°C$ change in temperature [21]. Moreover, temperature in the oral cavity constantly varies from $0°$ to $55°C$ depending on food and beverage intake [22]. Due to the fact that minor temperature changes cause insignificant contact angle changes and that the oral cavity does not have a consistent temperature, the influence of temperature on contact angle will be disregarded in this work. All materials used in this experiment will be maintained at a room temperature of $69°F$ for consistency.

2.2.1 Contact Angles of Water

In this work, the calibration of the goniometer is accomplished by measuring the contact angle of water on a glass plate and on a polytetrafluoroethylene (PTFE) specimen. A water contact angle less than $90°$ corresponds to wettability of the material. Low contact angles indicate that the solid material is hydrophilic to the liquid and the liquid will spread over the surface area. On the other hand, a water contact angle greater than $90°$ corresponds to hydrophobic solid material and indicates low wettability of the material [23]. The liquid will form a compact drop that does not spread over the solid surface. Complete wetting of a material will occur when the contact angle is $0°$ [18]. According to Sklodowaka *et al.*, the contact angle of distilled water on a glass plate is $51.05° \pm 0.84°$, therefore indicating hydrophilic material [24]. The contact angle of distilled water on PTFE is about $100°$, indicating a hydrophobic material [25].

Although this work is the first to measure the contact angle of artificial saliva on dental crown materials, contact angle measurements on impression and resin-based dental restorative materials are common in research [17, 26–28]. Menees *et al.* evaluated the contact angle of water and saliva on seven unset elastomeric impression materials in order to determine whether or not the materials are hydrophilic or hydrophobic. Ideal dental impression material should be hydrophilic. Menees used 5 μL drops of distilled water or saliva and dispensed them on the surface of flattened materials for 25 seconds. Contact angle measurements were obtained using a goniometer and measurements were taken at t_0, $t_1 = 2$ seconds, $t_2 = 5$ seconds, $t_3 = 50\%$ of working time, and $t_4 = 95\%$ working time of the material. The working time of the material is the time period between the start of the impression material preparation to the final time in which the material can be seated in the mouth of a patient without distortion. This time period is 45 seconds. The results of that study indicated that all materials were indeed hydrophilic [27]. Abdelsalam *et al.* used a similar procedure on cured impression material. A 5 μL drop of water was used and contact angle measurements were taken every 10 seconds for a total of 50 seconds. The results of that study showed that the impression materials were hydrophilic as well [28]. Therefore, for this study, the same method will be used to measure the contact angle on the crown materials.

2.3   Dental Crowns

Implants, crowns, and restorations are common in dentistry. The role of dental crowns is to minimize degradation by protecting weak teeth from breaking or wearing, restore broken teeth, or support teeth with fillings. Degradation of teeth may lead to periodontal diseases, temporo-mandibular disorders, loss of contact between opposing teeth, which is also known as loss of centric occlusion, diagonal teeth, functional route change during chewing, or masticatory muscle fatigue [3]. Moreover, extensive loss of the hard tissues on teeth caused by wear may lead

to reduced masticatory efficiency, exposed dentin, and exposure of the tooth pulp [6]. Therefore, minimizing tooth degradation is crucial for oral health.

There are many different types of dental crown materials that fall into four basic categories: metal, ceramic, porcelain, and zirconia. Metal crowns are usually gold alloy crowns. Metals are high in strength and can withstand the forces in the mouth that cause chipping. Gold is durable and is the least reactive type of material used in dentistry [29]. However, metal crown materials are not aesthetic and are no longer commonly used. Ceramics are crystalline materials composed of metal oxides. The metal oxides are formed by firing clays, also known as induced crystallization. Ceramics are highly brittle, opaque materials with high compressive strength and low tensile strength. These materials are used in dental crowns because they are metal free, biocompatible with soft tissue, and provide low plaque adherence. However, their low tensile strength makes fractures in restorations more likely to occur [29]. Porcelains are glass materials with crystalline fillers. The crystals in the porcelains add strength to the material and opacity by providing deep light scattering centers. Porcelains do not conduct heat well, which leads them to reduce temperature sensitivity in oral application. Porcelain crowns are usually covered with a surface glaze to increase surface strength. These materials produce a natural tooth-like coloring, and are therefore primarily used on front teeth for cosmetic purposes. However, porcelain materials are brittle and may fracture easily when they are exposed to resultant forces of grinding. Composite, or resin nano-ceramic, dental materials are a synthetic resin material that are usually used for tooth fillings, but can also be used for partial or full crowns. These materials have a high wear rate, especially when compared to natural tooth. Composites are used because they are less expensive than other types of crown material [29].

Due to the drawbacks of metal, ceramic, and porcelain crown materials, zirconia material was introduced. Zirconia crowns have higher deflection and fracture strength than conventional dental ceramics [30]. They have a translucent color which blends in well with the other teeth. But, zirconia crown materials have also been shown to be prone to chipping and cracking [31]. Currently,

ceramic, porcelain, and zirconia crowns are all still commonly used, depending on what the dentist prefers and which tooth needs restoration.

2.3.1 CAD/CAM Materials

The introduction of sophisticated and more precise processing of dental materials has been made possible with the creation of the computer-aided design and computer-aided manufacturing (CAD/CAM) technology [32]. CAD/CAM technology is used for creating dental restoration materials such as crowns, dentures, and fixed bridges. CAD/CAM dental materials are usually composed of a ceramic or composite solid blocks. Dentists must take a digital impression, or image scan, of the tooth needing the restoration. The digital impression is imported into a computer software. Missing areas of the tooth is virtually created on the software and the data is sent to a milling machine to be milled out of the solid ceramic or composite block. The milled material is then used for restoration in the patient's mouth [32]. Most dental crown materials used in this work are CAD/CAM materials.

2.3.2 Dental Wear

In dentistry, dental wear is defined as tooth surface damage or tooth loss caused by the direct contact between opposing teeth, or between teeth and opposing restorative material. Dental wear is a result of complex chemical and mechanical processes that occur in oral environments and is primarily dependent on age. The prevalence of wear increases from 3% to 17% from age 20 to 70 years [33]. Due to the differences in material properties, restorative materials tend to accelerate wear rates of antagonist teeth, causing excessive wear on the enamel. Excessive wear on enamel surfaces may cause abnormal loading that can result in clinical problems such as periodontal diseases, dentine hypersensitivity, or tooth death [31, 34].

Over the last few years, the introduction of higher hardness dental crown materials, such as zirconia, leucite-reinforced glass-ceramic and lithium disilicate glass-ceramic crowns, has stimulated

discussion and new studies regarding the damage and wear dental materials cause on the natural antagonist tooth [35]. Etman *et al.* showed the wear depth of teeth caused by ceramic crowns after implantation at 6, 12, 18, and 24 months. For example, wear in opposing natural teeth 12 months after the use of a ceramic crown was 149.7 μm and after 24 months it was 214.86 μm [36]. In another study, Stober *et al.* evaluated the enamel wear caused by zirconia crowns on opposing teeth and compared it to the natural wear caused by antagonist teeth. Twenty full molar zirconia crowns were implanted in twenty different patients with similar dental conditions. Impressions of both jaws were made before and six months after crown cementation in order to measure wear. Occlusal wear, or wear caused by the contacting surfaces between teeth, was measured with a 3D laser scanner. The results found that zirconia crowns were associated with greater wear (mean vertical loss of 33 μm on opposing enamel after 6 months) and degradation of the opposing enamel compared to the wear caused by the contralateral natural opposing teeth (mean vertical loss of 10 μm on opposing enamel after 6 months) [30]. This and other similar studies suggest that damage of tooth is due to the surface structure and roughness of the crown material [31, 34, 37–39].

The motivation behind this project is that dental crown materials may inhibit the lubrication function of saliva. The inhibition therefore causes wear and tooth decay, rather than the inherent surface roughness of the crown material as suggested by literature. This work will provide experimental results that investigate the effect of lubrication on different crown materials.

Wear Caused by Specific Crown Materials

The studies in this section provide wear data on the materials used in this research study. Those materials include: lithium disilicate glass-ceramics, leucite-reinforced glass-ceramics, resin nano-ceramics, feldspathic porcelains, and zirconia dental crown materials.

Silva *et al.* evaluated the volume of wear on opposing natural teeth caused by a lithium disilicate glass-ceramic and a leucite-reinforced glass-ceramic. Casts of the teeth were taken before and after crown material implantation. A 3D laser scanner was used to provide the images in the

wear value calculations. The results show that after three years of implantation, the lithium disilicate glass-ceramic material had overall wear on natural opposing tooth of 0.80 mm^3 while the leucite-reinforced glass-ceramic material had overall wear on natural tooth of 1.02 mm^3 [40].

Jung *et al.* evaluated the volumetric antagonist tooth wear caused by zirconia and feldspathic porcelain crown materials. Material specimens were created and embedded on extracted premolars. All specimens underwent wear testing via a chewing simulator that simulated the vertical and horizontal movements in the mouth. One year of chewing conditions is simulated by applying 240,000 loading cycles. The results showed that the feldspathic porcelain caused a 0.119 ± 0.059 mm^3 wear on natural opposing teeth while the zirconia caused 0.031 ± 0.033 mm^3 on the opposing natural teeth [34].

In a similar study, Preis *et al.* evaluated the wear caused by resin nano-ceramic and porcelain crowns. Steatite spheres made of magnesium silicate were used as antagonists in this study. The use of steatite spheres, is commonly used as a valid antagonist in in-vitro wear studies rather than natural enamel. Loading cycles of 120,000 cycles were applied to the specimen at a frequency of 1.6 Hz. The results showed that the resin nano-ceramic material caused 1.274 ± 0.379 mm^3 depth wear on the antagonist [41]. In 2015, Dupriez *et al.* applied a wear test with 50,000 loading cycles and found that the depth wear of a steatite antagonist against the resin nano-ceramic material was 55.4 ± 4.0 μm compared to 28.7 ± 9.0 μm caused by the leucite-reinforced glass-ceramic material [35].

In 2016, Nakashima *et al.* evaluated the antagonist enamel depth and volume loss against a lithium disilicate glass-ceramic, zirconia, and a feldspathic porcelain. The authors used flattened enamel antagonists and used a wear testing device. Loading cycles of 100,000 were applied with a 1.2 Hz frequency for each specimen. The results showed that the enamel had a depth of loss of 133.9 μm and a volume loss of 0.33 mm^3 against the lithium disilicate glass-ceramic, a depth of loss of 186.0 μm and a volume loss of 0.62 mm^3 against the feldspathic porcelain, and a depth of loss of 104.6 μm and a volume of loss of 0.07 mm^3 against the zirconia [42].

CHAPTER 3

GONIOMETER EXPERIMENTS

3.1 Goniometer Materials and Methods

This chapter discusses the experimental portion of this work. The different materials used in this method are listed in Section 3.1.1 and their preparations are explained in Section 3.1.2. The experimental method as well as the data analysis approach are also explained in Sections 3.1.3 and 3.1.4.

3.1.1 Dental Materials

The following dental crown materials were used:

- IPS e.max CAD (Ivoclar Vivadent AG, Schaan / Liechtenstein)

- IPS Empress CAD (Ivoclar Vivadent AG, Schaan / Liechtenstein)

- Celtra Duo (DENTSPLY International, DENTSPLY Prosthetics, York, Pennsylvania)

- Lava Ultimate CAD/CAM (3M, ESPE, United States)

- VKM (VITA, North America)

E.max CAD is a lithium disilicate glass-ceramic based crown material. E.max CAD has a flexural strength of 360 MPa and has desirable aesthetic characteristics, such as tooth color, translucency and brightness. Empress CAD is a leucite-reinforced glass-ceramic and has a flexural strength of 160 MPa. It is used due to its highly aesthetic restorations and its adaptation to natural tooth

color. Celtra Duo is a zirconia reinforced lithium silicate ceramic crown material. It has an flexural strength of 420 MPa. It is used due to its high level of translucency and opalescence. Lava Ultimate is a resin nano-ceramic material that combines glass ceramic and resin material properties. The ceramic particles consist of fillers of silica and zirconia materials. Lava has a flexural strength of approximately 200 MPa and is primarily used for filling restorations. It should be noted that in 2015, 3M ESPE recalled Lava Ultimate dental material from use for full crowns due to potential debonding of the material, which could cause tooth degradation. The Lava material is used in this work as a means of comparison among the other materials. VKM is a feldspathic porcelain material also used for crowns. It is simple in handling and firing, which makes it beneficial to use for layering restorations [43]. The artificial saliva used in the experiment is Biotene (GlaxoSmithKline, Moon Township, Pennsylvania).

3.1.2 Crown Material Preparation

Specimens of the VKM material were made manually by mixing the dry powder material with its specific solvent. The specimens were placed in the VITA Vacumat 6000 MP furnace, a fully-automatic, microprocessor-controlled firing unit. Material specimens were fired up according to their required temperatures as stated under their manufacturing guidelines. Firing of the material allows crystallization of maximum strength. After the firing process, the materials were left to cool and then polished using deluxe silicone wheels (Keystone Industries, Myerstown, PA). A glaze was applied to the material and each specimen is put back into the furnace. Glaze specifications are further discussed in Section 3.1.3. The CAD/CAM materials (e.max, Empress, Lava and Celtra Duo) were placed into a CAD/CAM machine and cut with a diamond blade. Each material was cut to create two specimen. Specimen were first polished by hand using a 500 and 1000 grit sandpaper (Wet/Dry Sandpaper Sheets, Warrior, Camarillo, CA), then polished again using the deluxe silicone wheels. According to the e.max CAD handbook (Ivolclar Vivadent), e.max specimens have to be fired up and glazed for maximum strength to be achieved. The e.max specimen were fired

in the vacumat furnace and glazed with the e.max CAD Crystal/Glaze Liquid (Ivoclar Vivadent, Liechtenstein). After preparation, all materials were stored in a cabinet at room temperature.

3.1.3 Experimental Method

In this section, the goniometer methods, sampling considerations, and goniometer data analysis will be discussed.

Goniometer

Before making measurements on crown material, the goniometer method must be validated by measuring the contact angle of water on PTFE and a glass microscopic plate. The first step of validation is demonstrating that contact angle measurements are similar to published results. The next step of validation is to demonstrate that any location on a specimen will yield approximately the same contact angle. Drops were measured on five different locations on a specimen, one at a time.

The methods used to determine the contact angle for each experiment is the same. A summary flowchart of the experimental process is shown in Figure 3.1. The Ramé-Hart Drop Image Software is linked to the goniometer, and provides the angle measurements. A specific liquid material and solid material were selected for each experiment (*i.e.* water and glass). Experimental parameters were then defined to obtain an angle measurement every 10 seconds for 50 seconds for a total of five measurements.

The goniometer configuration is shown in Figure 3.2. The goniometer is composed of a specimen platform, a micro-syringe, and a camera that is connected to the software. The small solid specimen was placed in the center of the platform and the camera was adjusted until a clear view was obtained. The image appears on the computer. One drop of liquid was then dispensed from the micro-syringe, but not allowed to drop from the needle. The specimen platform was raised up so the drop can settle on the specimen, then the platform was returned to its original spot. This

technique helps minimize extra drops from landing on specimen and was utilized in a prior study [17]. In the software, a vertical line is adjusted to define the center of the drop, and a horizontal line was adjusted to define the bottom of the drop, as seen in Figure 3.3. These lines define the drop and indicate where the angle measurements will be taken as seen in Figure 3.4. After the drop geometry is defined, the experiment is initiated.

Sampling Considerations

In this study, the term specimen is used for the solid material (the crown material, PTFE, or microscope plate). A liquid is either the water or artificial saliva. A trial is defined as the contact angle measurements obtained from one set of liquid-solid pair at a given time. In each trial, there are 5 angle measurements taken every 5 seconds. The goniometer records both the left and right angles, providing a total of 10 angle measurements over 50 seconds per trial. Trials are repeated three times on a given day, for a total of four days. Each day is considered a round.

Glaze

The glaze used for these materials is the e.Max CAD Crystal/Glaze Liquid (Ivoclar Vivadent AG, Schaan/Liechtenstein). When materials are first fired, the surface is matte, because the CAD/CAM grinder does not provide a polished finish. In order to get a high gloss on the surface of these materials, the glaze is applied on the surface which provides a thin layer of glass or porcelain. This glossy finish resembles the human enamel and provides a natural appearance to the crown material. The surface glaze also strengthens a material by closing surface defects found in materials.

3.1.4 Goniometer Data Analysis

The mean angle measurements for each trial was taken. For instance, for trial 1, there are ten angle measurements total. The mean of those ten measurements is the angle measurement representative of that trial. Results were analyzed using one-way ANOVA and Tukey-Kramer (α=0.05) methods on the JMP software. Prior studies on contact angles used those statistical tests for data
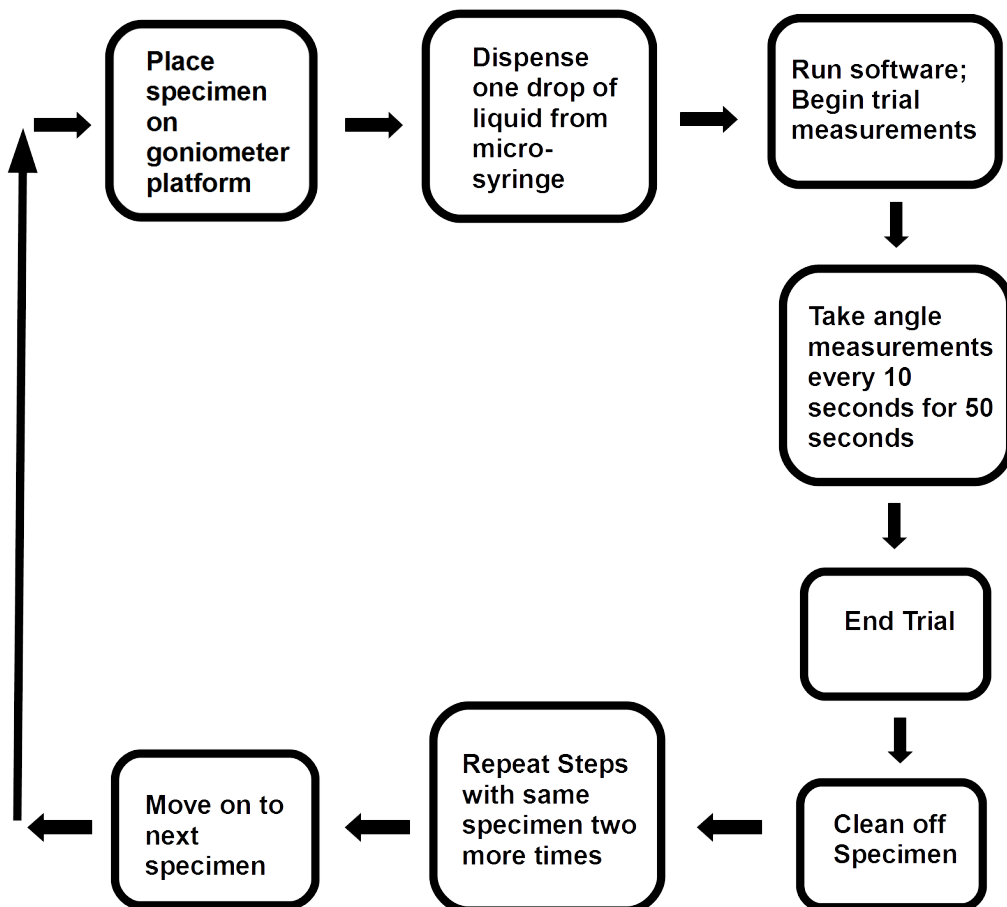
Figure 3.1: The flowchart above represents the experimental process taken to measure the contact angle using the goniometer. The process starts with the placement of a specimen on the goniometer platform and ends when three trials have occurred on the same specimen. The process is then repeated with a new specimen.
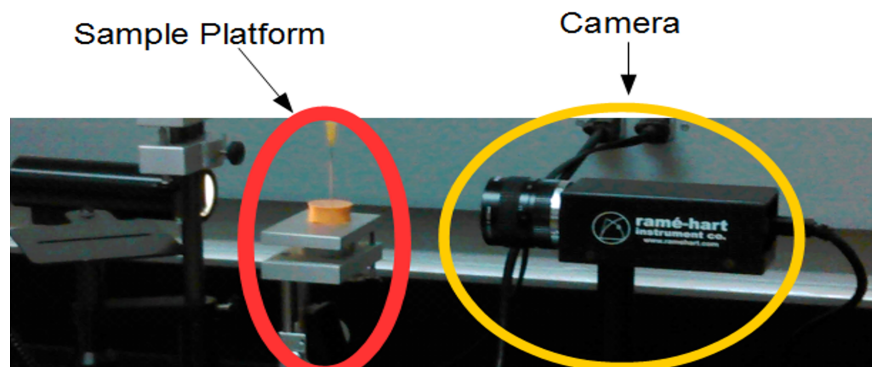
Figure 3.2: This is a photograph of the goniometer setup. The solid specimen is put on the platform, a drop of liquid is dispensed, and the camera captures an image of the liquid drop on the solid specimen. The contact angle is determined on the software and the photo is saved for MATLAB processing.

Figure 3.3: This image shows how a goniometer image is set up on the software. The solid rectangular surface is the solid material. The half circle represents the drop of liquid material. The top floating rectangle is the micro-syringe. The vertical dashed line indicates the center of the drop. The horizontal dashed line indicates the bottom of the drop. These lines are used for reference to measure the contact angle.

Figure 3.4: This image shows where the left and right contact angles (θ) are measured by the goniometer software.
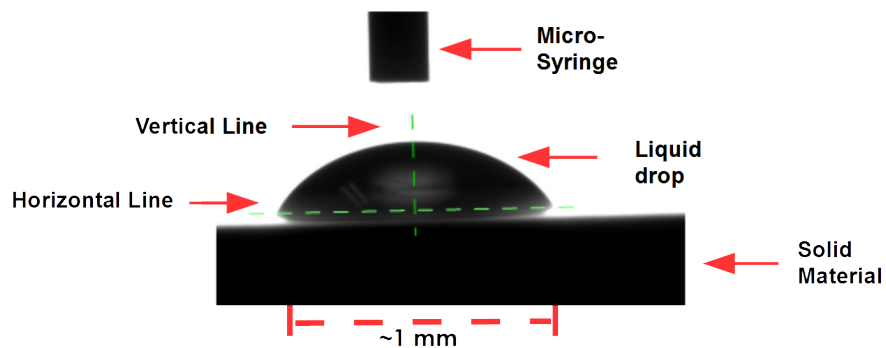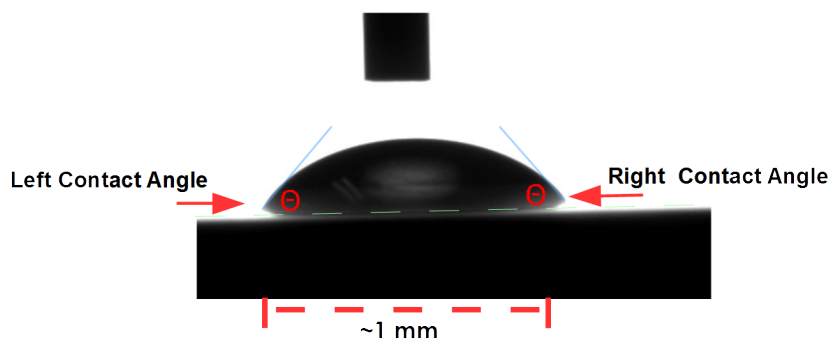
analysis [17, 27]. One-way ANOVA analysis tables were generated to analyze contact angle measurements of water by material, contact angle measurements of water by round, contact angle measurements of Biotene by material, and contact angle measurements of Biotene by round. In the JMP software, contact angle measurements were considered continuous numeric data while rounds and materials were considered "characters". The Tukey-Kramer (α=0.05) method was applied to each one-way analysis table which generated the circles on the right side of the tables. Each material was represented with a circle. If the circles of two groups did not overlap, or overlapped and had an external angle of intersection less than 90 degrees, then the two groups were significantly different. If the circles had a large overlap, then they were not significantly different. This method also provided a report that labels statistically similar materials by the same letter. Box-plots were created on each one-way analysis and are presented in Figures 3.5-3.9.

3.2   Goniometer Results

Figures 3.5-3.9 present the one-way analysis tables obtained from the JMP software. All Figures are explained in Sections 3.2.4-3.2.7.
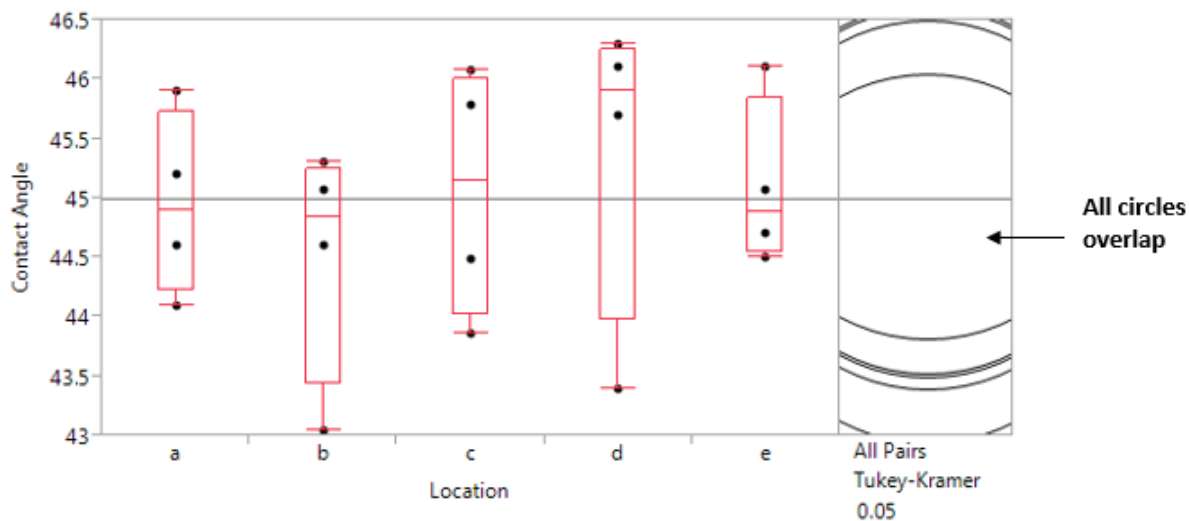
Figure 3.5: The ANOVA plot shows the contact angle of water on five different locations on empress material specimen. The box-plots represent the IQR for each location. The circles on the right are a result of a Tukey-Kramer (α=0.05) application.

3.2.1 Drop Location

In order to determine whether or not the location of the drop affects the contact angle measurements, a drop was placed onto five different locations of the Empress material specimen and evaluated. These five locations included the four corners, and the center of the specimen. Figure 3.5 shows the one-way ANOVA plot with Tukey-Kramer (α=0.05) analysis. All circles overlapped indicating that there is no statistically significant (α=0.05) effect on contact angle measurements by drop location. Therefore, the location of the drop is independent of contact angle measurements.

3.2.2 Water and Artificial Saliva on Teflon

According to the goniometer, the contact angle of water on PTFE is 91.2°. This value is the result of averaging all data trials, which are presented in full in the Appendix. A water contact angle greater than 90° corresponds to hydrophobic solid material [23]. Literature indicates that

PTFE is a hydrophobic material and the contact angle of distilled water on PTFE is $100°$ [25]. The contact angle of water on PTFE is greater than that of all the tested material (Figure 3.6), indicating that PTFE is the most hydrophobic material. The contact angle of Biotene on PTFE is $61.68°$ as indicated by the goniometer. This angle value is the greatest value compared to that of the other tested materials presented in Figure 3.7. Although the angle value of Biotene is smaller than the angle value of water, it still shows that PTFE is the most hydrophobic material.

3.2.3 Water and Artificial Saliva on Glass Plate

The mean contact angle of water on a glass plate for all trials is $55.2°$. Again, this value is the result of averaging all data trials presented in the Appendix in Figure 7.1. Literature indicates that the contact angle of water on glass is $51.05° \pm 0.84°$ using a 5 μL drop size [24]. In this work, the drop size varied among different trials due to the manual nature of the goniometer's micro-syringe. The mean contact angle of Biotene on a glass plate for all trials is $40.4°$, which is less than that observed for water. As Biotene is meant to assist in the wetting of materials, it makes sense that the contact angle is lower than that of water.

3.2.4 One-way ANOVA Analysis of Contact Angle of Water by Material

Figure 3.6 presents the one-way ANOVA analysis of the contact angle of water by material. The circles on the right side of the one-way analysis table represent the Tukey-Kramer method. Circles that overlap indicate that certain materials are related and share the same material characteristics. Circles that are independent of others indicates that these materials are significantly different from others (α=0.05). Circles that do not overlap or have a small overlap are assigned distinct letters, indicating the materials are not similar. From this table, it is noted that PTFE has the greatest contact angle and is in its own distinct group represented by a letter 'A'. PTFE is the most hydrophobic material, and therefore, explains the distinct grouping. The contact angle of water on a glass plate shares a distinct group with the Lava material and they are represented by
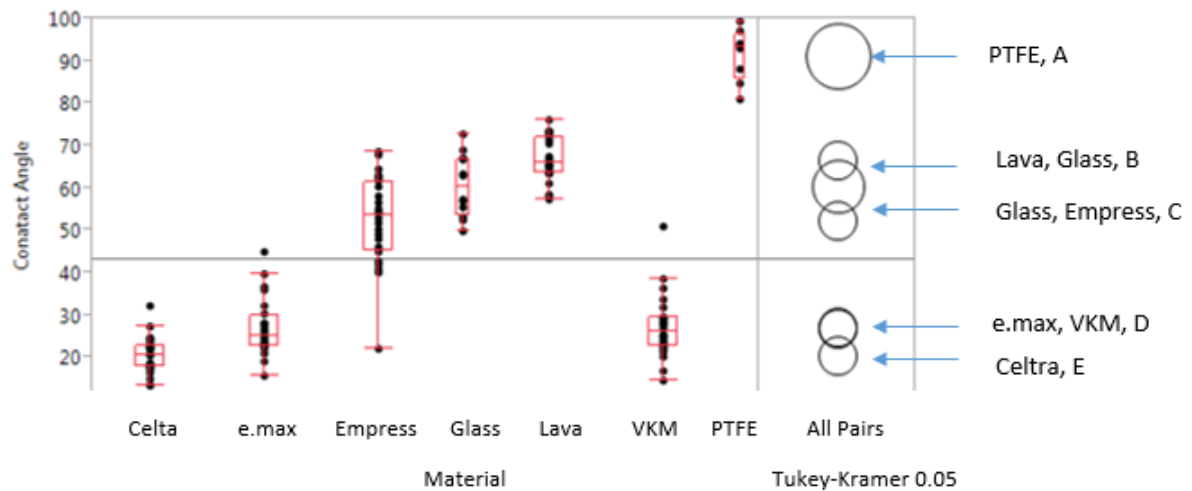
Figure 3.6: The one-way ANOVA plot shows the contact angle of water on every material. The box-plots represent the IQR for each material. The circles on the right are a result of a Tukey-Kramer application. Circles that have a small or no overlap are assigned a distinct letter to indicate statistical significance (α=0.05).
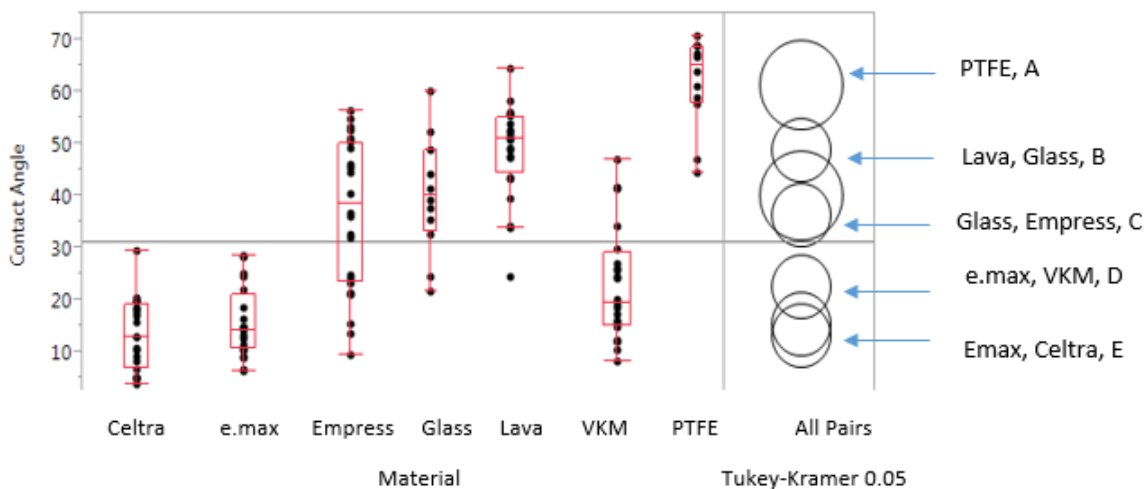
Figure 3.7: This one-way analysis plot shows the contact angle of Biotene on each material. Materials with no statistical significance are grouped by the same letter. These materials include Lava and glass, glass and Empress, e.max and VKM, and e.max and Celtra

the letter 'B'. This result indicates they are more closely related to each other. Lava has a mean contact angle measurement of 66° while glass has a mean contact angle measurement of 60°. The Empress material is in its own distinct group and it is represented by the letter 'C', because it shares a small overlap with glass, but no overlap with the other materials. It has a mean contact angle measurement of 52°, placing it right in the middle. The VKM and e.max materials also share a group and they are represented by the letter 'D'. Both materials displayed a mean contact angle of about 27°, hence their circles overlap in Figure 3.6. Celtra is in its own distinct group, represented by a letter 'E'. Celtra has the lowest mean contact angle measurement of 20°. This result indicates that Celtra is the most hydrophilic material.

3.2.5 One-way ANOVA Analysis of Contact Angle of Biotene by Material

Figure 3.7 presents the one-way ANOVA analysis of the contact angle of Biotene by material. The contact angle of Biotene on the materials shows a similar trend to that of water on the materials. However, more materials seem to have overlapping circles. PTFE again displayed the largest mean contact angle and is represented in its own group, 'A'. Lava and glass follow PTFE, and share the distinct group, 'B'. However, glass also shares a distinct group with the Empress material, 'C'. VKM and e.max displayed similar characteristics and are grouped in the distinct group, 'D'. The e.max material sample also shares a distinct group with Celtra, 'E'. Both e.max and Celtra have the lowest mean contact angle measurements with e.max being at $15°$ and Celtra being at $13°$. All angle measurements are significantly smaller compared to the angle measurements of water. This indicates that Biotene indeed displays strong wetting properties, and hence many materials start displaying statistically similar results.

3.2.6 One-way ANOVA Analysis of Contact Angle of Water by Round

Figure 3.8 presents the one-way ANOVA analysis of the contact angle of water by round. All circles overlap indicating that there is no statistically significant effect on contact angle measurements by the different rounds.

3.2.7 One-way ANOVA Analysis of Contact Angle of Biotene by Round

Figure 3.9 presents the one-way ANOVA analysis of the contact angle of Biotene by round. Again, all circles overlap indicating that there is no statistically significant effect on contact angle measurements by the different rounds.

Figure 3.8: This ANOVA plot compares the contact angle of water by round. All circles overlap indicating no statistical significance in round.
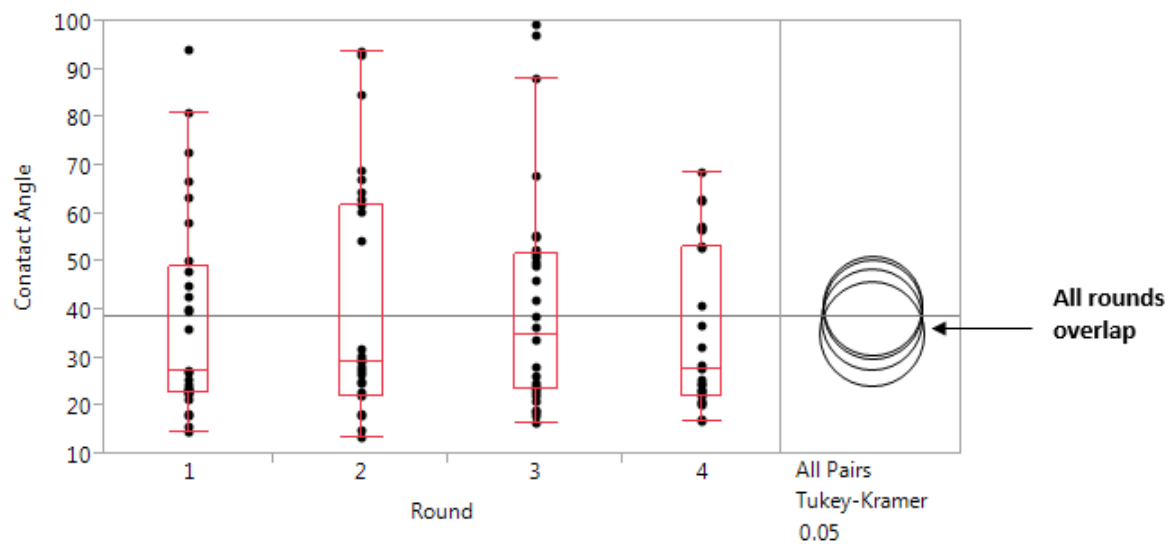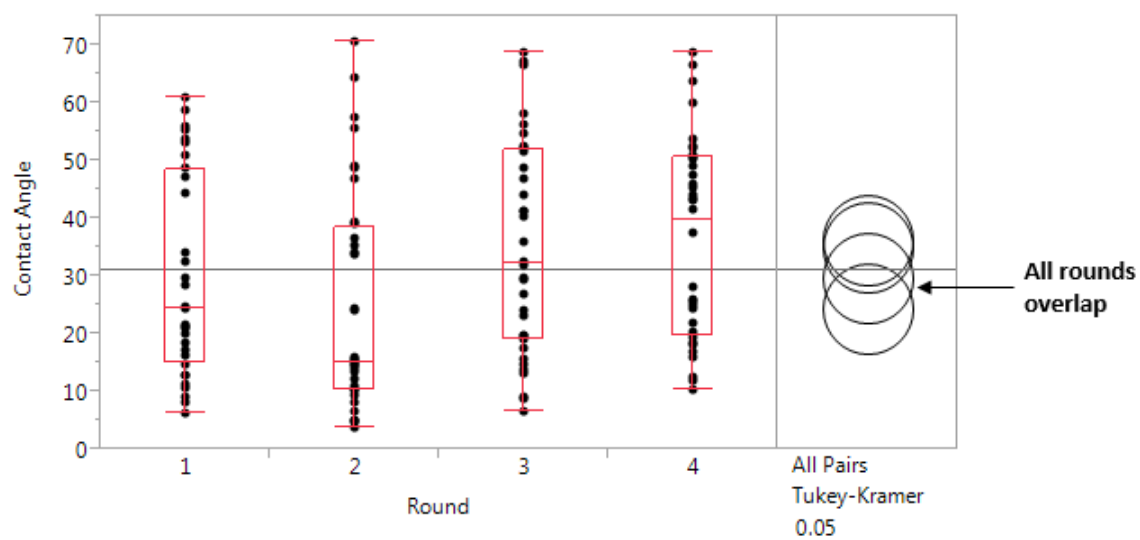
Figure 3.9: This ANOVA plot compares the contact angle of Biotene by round. All circles overlap indicating no statistical significance in round.

CHAPTER 4

MATLAB IMAGE PROCESSING

This chapter discusses the image processing code that was developed to complement the goniometer contact angle measurements. Sample images and results obtained from the code are also presented in this chapter.

4.1   Image Processing

Image processing refers to the steps taken to manipulate a digital image to extract certain features from it or to improve its overall quality. There are five main purposes of imaging processing and they are to visualize objects that are not visible, to make an image better by sharpening or restoring it, to retrieve an image, to measure other objects in an image, and to distinguish specific objects in an image. Processing can be applied to images in various disciplines, such as medicine, biometrics, astronomy, biology, military applications, satellite imagery, and dentistry. Most image processing systems treat images as two dimensional signals, and then apply set signal processing methods to them. Image processing requires only three steps. First an image is imported via an image acquisition tool. Then mathematical operations are done on the image in order to analyze and manipulate it. Finally, the new image or image of interest, is output [44].

In the image processing system, the image is the input, and the image characteristics are the output. An image can be a photograph or a video, but a computer would see it as an array or a matrix of square pixels arranged in columns and rows. Images are divided into pixels, where the number of pixels depends on the resolution of the image of interest. For black and white images,

or binary images, the image processing software will assign each pixel a value of 0 or 1. A value of 0 represents a complete absence of color, or white. A value of 1 represents full saturation of color, or black. MATLAB records each pixel value in a matrix. In a gray-scale image, each pixel value ranges from 0 and 255 indicating different levels, or shades of gray [44]. This work will use a series of algorithms to manipulate the goniometer image in order to determine the contact angle.

In this work, the input is the goniometer contact angle image obtained for a given trial. The desired output image characteristics include: an outline of the image, identification of desired pixels, and the development of a line that is used to determine the contact angle measurement.

4.2   Image Processing Software

The purpose of the MATLAB code was to find the contact angle of a drop of liquid on a material surface. First an image was imported from the goniometer into the MATLAB software (Figure 4.3 A). A threshold was set to create a binary image from the original gray scale image (Figure 4.3 B). Binary images allow for only two possible values for each pixel, black or white. For a black and white image, the image processing software will assign each pixel a value of 0 or 1. A value of 1 represents a complete absence of color, or white. A value of 0 represents full saturation of color, or black. The image is represented as a rectangular matrix of pixel values.

In order to apply edge detection, a mask was created. Masks are filters applied to the image. Sudden transitions in the image between black and white pixels are detected by the mask. In this work, a mask was created to search and find all the first black pixels in the image starting from the top most, left pixel, which corresponded to the outline of the drop (Figure 4.1). The resulting plot is a black outline of the drop of liquid on the material surface and is presented in Figure 4.3 C.

The next task was to find the most top most, center pixel on the drop (Figure 4.2). This pixel will be connected to the bottom corner pixel to form a line for trigonometry purposes. A series of algorithms were created to find this pixel. The first algorithm was created to find the first black

Figure 4.1: The mask was created to find the first black pixel in the image starting from the top, left as indicated by the search arrow.
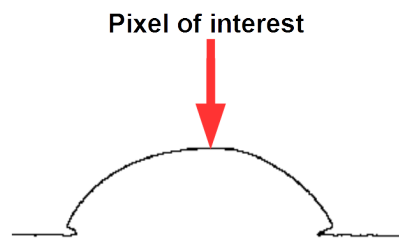
Figure 4.2: This pixel is the top most, center pixel. This pixel will be connected to the bottom corner pixel to form a line

pixel on the upper most area of the drop and marking it with a red X (Figure 4.4 D). The image was flipped left to right so that the same algorithm can be applied to find the first black pixel. This pixel was marked with a blue X and corresponds to the first black pixel on the right side of the drop outline (Figure 4.4 E). Both Xs were then plotted on the edge detected image (Figure 4.5 F). The midpoint between the two pixels is the pixel of interest, which is the top most center pixel. This pixel was marked with a green X (Figure 4.5 G).

Starting with the blue X on the far right portion of the drop image (Figure 4.4 E), an algorithm was created to check the neighboring four pixels for each pixel, until the corner pixel of the drop was reached. The desired corner pixel was characterized by having a top pixel of black, a right
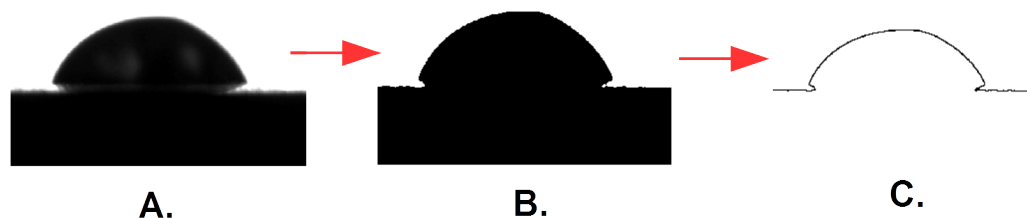
Figure 4.3: An image is imported from the goniometer software into MATLAB (A.) A threshold is set and the image is converted into a binary image (B.). The mask is applied to detect the edges and outline the drop (C.).

pixel of white, a bottom right pixel of white, and bottom pixel of white. Once all these criteria were met, the desired pixel was found and marked with a green X (Figure 4.6 H). A line was created by joining the two green X (Figure 4.6 I). To determine the angle, trigonometry was applied to the line by using inverse tangent function to find the angle of interest, which was the contact angle.

4.2.1   Sample Images

The sample images presented in Figures 4.3-4.6 show the progression through the MATLAB code. Each image corresponds to a different step in the MATLAB code and is labeled with a distinct letter.

4.3   MATLAB Results

For each liquid-material combination, two images were used for image processing. A table was created recording the goniometer angle value and the MATLAB angle value for each image (Figure A.3). Figure 4.7 provides a visual representation of the goniometer and MATLAB angle measurements. It can be seen that both the goniometer and the MATLAB code provided angle measurements that correlated except for a few measurements. Figure 4.8 presents the percent

C.   **D.**   **E.**
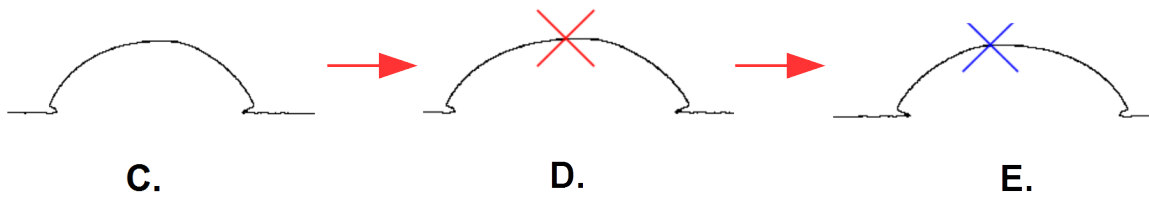
Figure 4.4: An algorithm is used to detect the first top most pixel on the left side of image C and marks it with a red X (D). Image C is flipped, and the same algorithm is used to detect the first top most pixel that is on the right side and marks it with a blue X (E). Both the Xs are now marked on image C (F).

E.   **F.**   **G.**
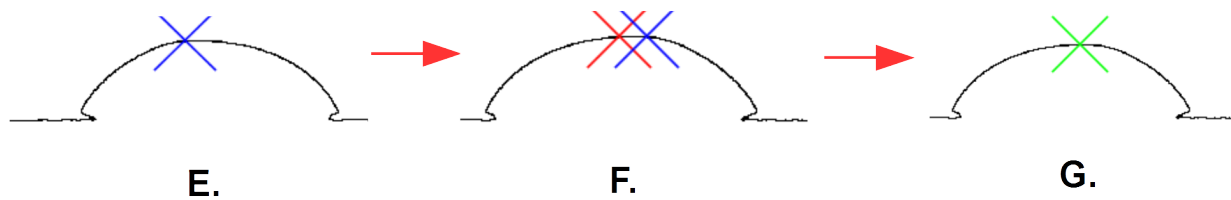
Figure 4.5: The top most middle pixel is found by finding the median value of the the left most and right most pixels and is marked with a green X (G).
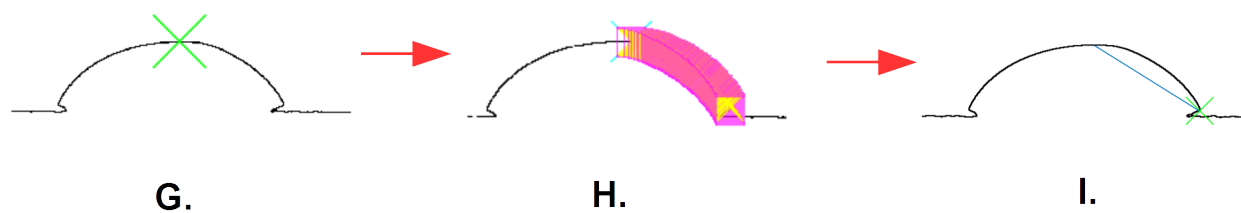
Figure 4.6: Starting from the pixel marked in image G, an algorithm is applied to search all the pixels on the right side of the drop to find the bottom right corner pixel (H). This pixel is marked by another green X. The two green Xs are connected to form a line (I). Trigonometry is applied to this line.

difference of contact angle by each of the measured specimen. Most specimens had a $\pm$ 10 percent difference except for three measured specimen.
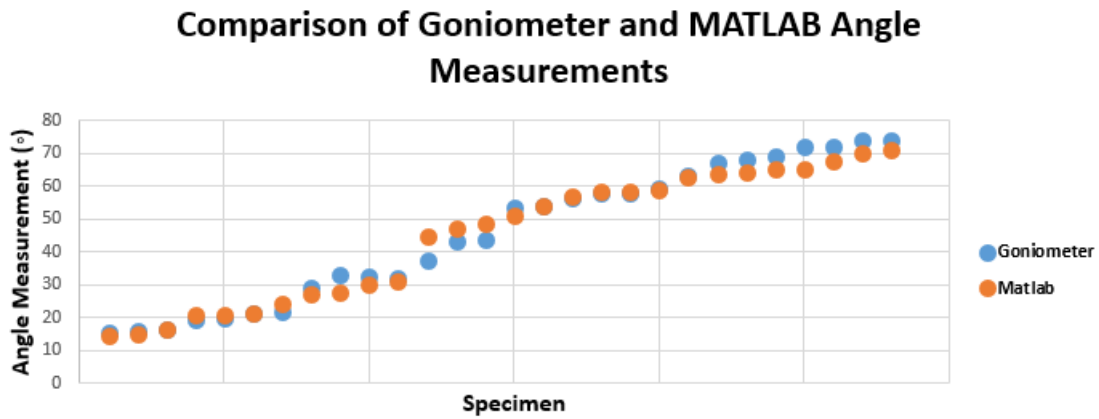
Figure 4.7: This figure plots the angle measurements from both the goniometer and MATLAB code for each specimen.
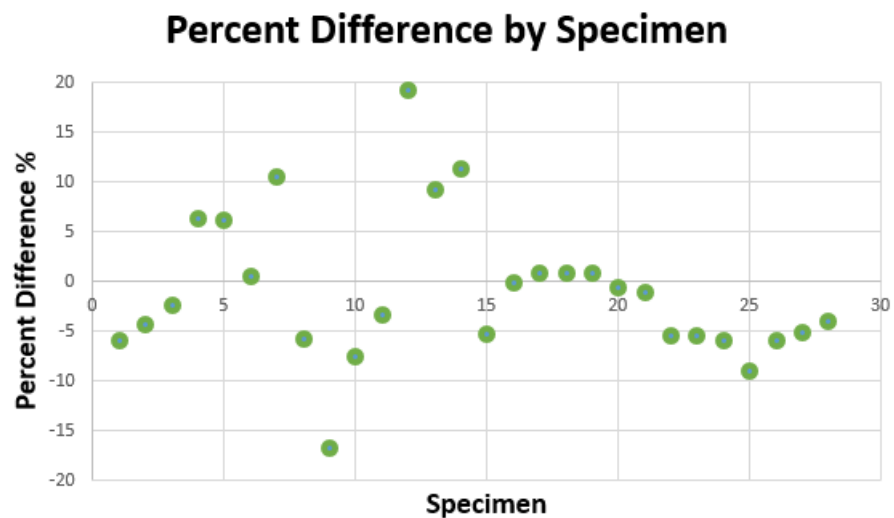
Figure 4.8: This figure plots the percent error for each specimen.

CHAPTER 5

DISCUSSION

The motivation behind this study is to evaluate the relative amount of lubrication saliva provides on dental crown material surfaces by measuring the contact angles for artificial saliva on dental materials. An image processing code was developed to complement the goniometer contact angle measurements.

5.1   The Contact Angle Method

In order to correlate contact angle measurements with wear on antagonist teeth caused by the specific crown materials used, wear data was gathered for relevant dental materials from studies published between 2010 and 2016 [34, 35, 40–42]. The materials for which wear data is available are: resin nano-ceramics [35, 41], leucite-reinforced glass-ceramics [35, 40], feldspathic porcelain [34, 42], lithium disilicate glass-ceramic [40, 42], and zirconia [34, 42].

Section 2.3.2 discusses the prior wear studies done on these crown materials. Table 5.1 presents a summary of the volume and depth wear data found in the literature. The materials presented in Table 5.1 are listed in order of decreasing contact angle as obtained from the experimental potion of this work. Wear data for each material differs from study to study, depending on the experimental conditions the authors used such as loading cycles, antagonist material, and/or years of implantation. Regardless of experimental parameters, the relative magnitude of wear reported in all of these studies is consistent with the ranking of the contact angle measurements.

Nakashima *et al.* is the most recent study and authors evaluated the volume and depth enamel loss caused by feldspathic porcelain, lithium disilicate glass-ceramic, and zirconia crown materi-

Table 5.1: Goniometer and Wear Data Summary

Material	Measured Contact Angle [°]	Enamel Volume Loss, mm^3	Loading Cycles	Enamel Depth Loss, μm	Comment
Resin Nano-Ceramic	48.9	1.274 ± 0.379 [41]	120,000	–	Steatite Antagonist
		–	50,000	55.4 ± 4.0 [35]	Steatite Antagonist
Leucite-Reinforced	36.5	–	50,000	28.7 ± 9.0 [35]	Steatite Antagonist
Glass-Ceramic		1.02 [40]	3 y *in vivo*	–	Natural Enamel
Feldspathic Porcelain	22.7	0.119 ± 0.059 [34]	240,00	–	Maxillary Premolars
		0.62 [42]	100,000	186.0 [42]	Flattened Enamel Antagonist
Lithium Disilicate	15.6	0.80 [40]	3 y *in vivo*	–	Natural Enamel
Glass-Ceramic		0.33 [42]	100,000	133.9 [42]	Flattened Enamel Antagonist
Zirconia	13.4	0.031 ± 0.033 [34]	240,000	–	Maxillary Premolars
		0.07 [42]	100,000	104.6 [42]	Flattened Enamel Antagonist

als. This 2016 study suggests that wear on antagonist teeth is greatest from feldspathic porcelain, followed by the lithium disilicate glass-ceramic, and the zirconia opposing crown material [42]. These wear data correlate with the contact angle measurements obtained from this work.

In 2015, Dupriez *et al.* evaluated the depth of enamel loss caused by the resin nano-ceramic and leucite-reinforced glass-ceramic crown material. Their results showed that the resin nano-ceramic caused more wear on opposing enamel than the leucite-reinforced glass-ceramic. The wear data values obtained from this study are lower than the wear data values obtained from Nakashima *et al.*, but this can be attributed to the different experimental condtions used [35].

Silva *et al.* evaluated the volume loss of enamel caused by lithium disilicate glass-ceramic and leucite-reinforced glass-ceramic crown material. The authors found that the leucite reinforced glass-ceramic caused more wear on opposing enamel than the lithium disilicate glass-ceramic. Furthermore, Preis *et al.* evaluated the enamel volume loss caused by the resin nano-ceramic material. The value obtained from this study is the greatest volume loss value obtained compared to all the other studies. Together, Dupriez *et al.*, Silva *et al.*, and Preis *et al.* suggest that the resin nano-ceramic material causes more wear on opposing antagonist, followed by leucite-reinforced glass-ceramic, and finally the lithium disilicate glass-ceramic crown material. The contact angle measurements obtained from this work correlates with these studies [35, 40, 41].

Overall, the wear values caused by these specific crown materials obtained from these literature sources correlate with the contact angle measurements. The resin nano-ceramics material caused the most wear on opposing tooth, followed by the leucite-reinforced glass-ceramics, then the feldspathic porcelain, then the lithium disilicate, and lastly the zirconia. These results are consistent with they hypothesis that the greater the contact angle of artificial saliva, the greater the wear on the natural opposing enamel, due to less salivary lubrication.

5.2   Normalization of Data

Wear values reported by literature were normalized in order to provide a more direct means of comparison. Literature reports wear values per a specific numbers of chewing cycle. Wear values were divided by their respective number of cycle to obtain a value of wear per cycle. For instance, Nakashima *et al.* reported a volume loss of 0.33 mm^3 after application of 100,000 chewing cycles [42]. This was normalized by dividing 0.33 mm^3 by 100,000 chewing cycles to obtain a value of 0.0000033 mm^3/cycle. Moreover, Jung *et al.* states that chewing cycles between 240,000-250,000 correlate with one year of chewing under typical clinical conditions [34, 45, 46]. Since Silva *et al.* reported depth loss after three years under clinical parameters, a value of 240,000 chewing cycles was used to normalize their data values [4]. Normalized depth and volume wear data were plotted by their respective author against contact angle values presented in Figure 5.1. Wear data from each author is plotted with a different symbol. Within Figure 5.1, there is a trend presented by every author and this trend is consistent by all authors. This trend is that materials that cause the most depth or volume wear on opposing antagonist, has the greatest contact angle measurement.

5.3   Experimental Sources of Error

Sources of error were identified throughout the goniometer portion of this work. The aim was to use a drop size of about 5 μL, which is approximately one drop from the micro-syringe. Due to the manual nature of the goniometer, this drop size was inconsistent within different trials and ranged by approximately $\pm$ 5 μL. Some liquids also wet the solid surfaces more quickly than others, and therefore, required a larger drop volume (multiple drops) in order to remain on the screen for the goniometer measurements to occur. Moreover, the surfaces of some of the crown material were not completely flat. Kugel *et al.* indicated that while surface heterogeneity and drop volume may result in different contact angle measurements, they do not lead alter the overall ranking in materials hydrophilic behavior. In other words, surface heterogeneity and drop size may have led

Effect of Contact Angle on Dental Wear
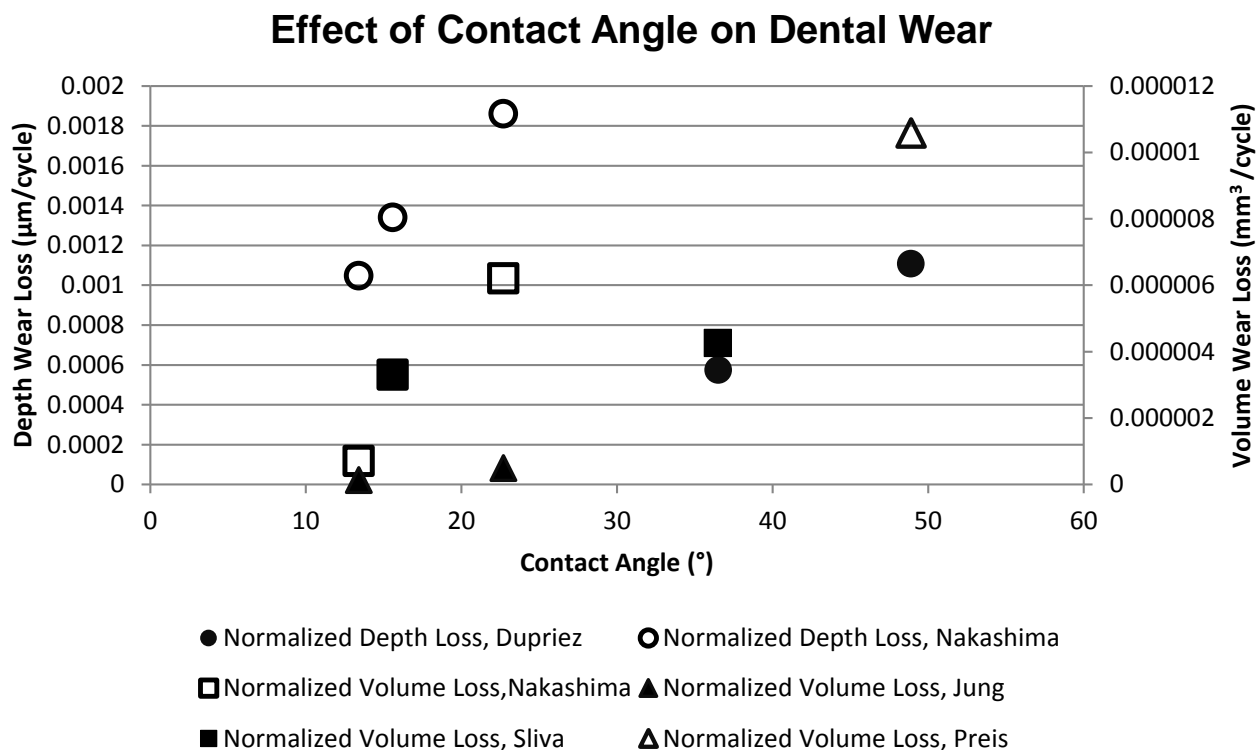
Figure 5.1: This graph plots the normalized volume and depth wear obtained from literature by each author versus the goniometer angle measurements. The trend within each author is consistent and is that materials that cause more depth or volume loss on opposing antagonist have higher contact angle values.

to different angle measurements within the same material, but they are not significant enough to effect the overall hydrophilic ranking of the materials.

5.4 Image Processing

The purpose of the MATLAB code was to complement the goniometer measurements. An image was imported from the goniometer into the MATLAB software. The gray scale goniomter image was converted into a binary image. Edge detection was applied by creating a mask to detect the first black pixels on the drop image, which resulted in outlining the drop of liquid (Figure 4.3). A series of algorithms were applied to the image in order to find specific pixels of interest (Figure

4.4). The end goal was to find the top most, center pixel on the drop and the bottom, right corner of the drop, and to connect the two pixels with a line (Figures 4.5 and 4.6). This line would be used as a trigonometry reference to measure the contact angle. Two images were selected for each solid-liquid combination to be evaluated yielding 28 total images. The results from this work show that MATLAB angle measurements correlated with the goniometer angle (Figure 4.7). The angle percent difference for each liquid-solid combination was evaluated. The percent difference for each combination fell within ± 20 percent (Figure 4.8). There were only three liquid-solid combinations that yielded a large percent difference. Those included Biotene on e.max and Empress, and water on VKM.

CHAPTER 6

CONCLUSIONS

Dental crowns are a major component of restorative dentistry. Literature indicates that these crown materials cause wear on the natural opposing tooth. The idea behind this work is that lack of salivary adherence on the crown materials contributes to the wear. This work evaluated the presence of salivary lubrication on dental crown materials by measuring the contact angle of water and saliva on a selection of crown materials. A goniometer was used for experimental angle measurements and an image processing code was developed using MATLAB software to complement goniometer measurements. The following dental crown materials were evaluated: resin nano-ceramics, leucite-reinforced glass-ceramics, feldspathic porcelain, lithium disilicate glass-ceramic, and zirconia. The results from this work show the resin nano-ceramics material is the most hydrophobic dental crown material with a contact angle of $60.5°$, while zirconia is the most hydrophilic material with a contact angle of $20.4°$. MATLAB angle measurements correlated with the goniometer angle measurements. Measured contact angles correlate with wear data from literature and show the trend that both depth and volume wear loss on antagonist teeth increases as contact angle increases. This indicates that lack of salivary adherence on the dental crown material will cause greater wear on the natural opposing tooth. Contact angle measurements and wear caused by these crown materials decreases from most to least as follows: resin nano-ceramics, leucite-reinforced glass-ceramics, feldspathic porcelain, lithium disilicate glass-ceramic, zirconia.

REFERENCES

[1] Y. Lee and J. Powers. Influence of salivary organic substances on the discoloration of esthetic dental materials-A review. *Journal of Biomedical Materials Research Part B: Applied Biomaterials*, 76B(2):397–402, February 2006.

[2] A Barrantes, T Arnebrant, and L Lindh. Characteristics of saliva films adsorbed onto different dental materials studied by QCM-D. *Colloids and Surfaces A: Physicochemical and Engineering Aspects*, 442:56–62, February 2014.

[3] M. Kaplan and B. Baum. The functions of saliva. *Dysphagia*, 8(3):225–229, 1993.

[4] A. Silva, S. Junio, L. Baratieri, E. Araujo, and N. Widmer. Dental Erosion: Understanding This Pervasive Condition. *Journal of Esthetic and Restorative Dentistry*, 23(4):205–216, August 2011.

[5] D. Veeregowda, H. Mei, J. Vries, M. Rutland, J. Valle-Delgado, P. Sharma, and H. Busscher. Boundary lubrication by brushed salivary conditioning films and their degree of glycosylation. *Clinical Oral Investigations*, 16(5):1499–1506, December 2011.

[6] E. Reeh, W. Douglas, and M. Levine. Lubrication of saliva substitutes at enamel-to-enamel contacts in an artificial mouth. *The Journal of Prosthetic Dentistry*, 75(6):649–656, June 1996.

[7] X. Wang, K. Kato, and K. Adachi. The Lubrication Effect of Micro-Pits on Parallel Sliding Faces of SiC in Water. *Tribology Transactions*, 45(3):294–301, January 2002.

[8] L Ma and W. M. Rainforth. The effect of lubrication on the friction and wear of Biolox delta. *Acta biomaterialia*, 8(6):2348–2359, 2012.

[9] L. Guo, P. L. Wong, and F. Guo. Correlation of Contact Angle Hysteresis and Hydrodynamic Lubrication. *Tribology Letters*, 58(3):45, May 2015.

[10] JL Barrat and L Bocquet. Large Slip Effect at a Nonwetting Fluid-Solid Interface. *Physical Review Letters*, 82(23):4671, June 1999.

[11] L. Gao and T. McCarthy. Contact Angle Hysteresis Explained. *Langmuir*, 22(14):6234–6237, July 2006.

[12] D. Kwok and A. Neumann. Contact angle measurement and contact angle interpretation. *Advances in colloid and interface science*, 81(3):167–249, 1999.

[13] F. Guo, S. Y. Yang, C. Ma, and P. L. Wong. Experimental Study on Lubrication Film Thickness Under Different Interface Wettabilities. *Tribology Letters*, 54(1):81–88, February 2014.

[14] P. Letellier, A. Mayaffre, and M. Turmine. Drop size effect on contact angle explained by nonextensive thermodynamics. Young's equation revisited. *Journal of Colloid and Interface Science*, 314(2):604–614, October 2007.

[15] A Amirfazli, D. Kwok, J. Gaydos, and W. Neumann. Line Tension Measurements through Drop Size Dependence of Contact Angle. *Journal of Colloid and Interface Science*, 205:1–11, April 1998.

[16] J Gaydos and W Neumann. The Dependence of Contact Angles on Drop Size and Line Tension. *Journal of Colloid and Interface Science*, 120(1):76–86, November 1987.

[17] G. Kugel, T. Klettke, J. Goldberg, J. Benchimol, R. Perry, and S. Sharma. Investigation of a new approach to measuring contact angles for hydrophilic impression materials. *Journal of Prosthodontics*, 16(2):84–92, 2007.

[18] Y. Yuan and R. Lee. Contact Angle and Wetting Properties. In G. Bracco and B. Holst, editors, *Surface Science Techniques*, volume 51, pages 3–34. Springer Berlin Heidelberg, Berlin, Heidelberg, 2013.

[19] R. Karmouch and G. Ross. Experimental Study on the Evolution of Contact Angles with Temperature Near the Freezing Point. *The Journal of Physical Chemistry C*, 114(9):4063–4066, March 2010.

[20] J. Bernardin, I. Mudawar, C. Walsh, and E. Franses. Contact angle temperature dependence for water droplets on practical aluminum surfaces. *International Journal of Heat and Mass Transfer*, 40(5):1017–1033, March 1997.

[21] D.R. Palamara, T. Neeman, A.N. Golab, and A. Sheppard. A statistical analysis of the effects of pressure, temperature and salinity on contact angles in CO2-brine-quartz systems. *International Journal of Greenhouse Gas Control*, 42:516–524, November 2015.

[22] C. Figueiredo-Pina, A. Monteiro, M. Guedes, A. Mauricio, A.P. Serro, A. Ramalho, and C. Santos. Effect of feldspar porcelain coating upon the wear behavior of zirconia dental crowns. *Wear*, 297(1-2):872–877, January 2013.

[23] R. Forch, K. Graf, and M. Kappl. Surface Design: Applications in Bioscience and Nanotechnology. In *Physics and chemistry of interfaces*, Physics textbook. Wiley-VCH, Weinheim, 2003. OCLC: ocm52623154.

[24] A. Sklodowaka, M. Wozniak, and R. Matlakowska. The method of contact angle measurements and estimation of work of adhesion in bioleaching of metals. *Biological Procedures Online*, 1:114, May 1998.

[25] J Cho. Polymer Surface Modification: Relevance to Adhesion. In *Polymer Surface Modification: Relevance to Adhesion*, volume 3. August 2004.

[26] S. Ruttermann, T. Beikler, and R. Janda. Contact angle and surface free energy of experimental resin-based dental restorative materials after chewing simulation. *Dental Materials*, 30(6):702–707, June 2014.

[27] T. Menees, R. Radhakrishnan, L. Ramp, J. Burgess, and N. Lawson. Contact angle of unset elastomeric impression materials. *The Journal of Prosthetic Dentistry*, 114(4):536–542, 2015.

[28] R. Abdelsalam and de R. Waldemar. Contact Angle of Water on Silicone Containing Impression Materials. *45th Annual Meeting of the American Association on Dental Research*, March 2016.

[29] M Rich. A Comparison of Dental Crown Materials, 2014.

[30] T. Stober, J. L. Bermejo, P. Rammelsberg, and M. Schmitter. Enamel wear caused by monolithic zirconia crowns after 6 months of clinical use. *Journal of Oral Rehabilitation*, 41(4):314–322, April 2014.

[31] R. Hmaidouch and P. Weigl. Tooth wear against ceramic crowns in posterior region: a systematic literature review. *International Journal of Oral Science*, 5(4):183, December 2013.

[32] T. Miyazaki, Y. Hotta, and J. Kunii. A review of dental CAD/CAM: current status and future perspectives from 20 years of experience. *Dental Materials Journal*, 28(1):44–56, 2009.

[33] V Spijker and JM Rodriquez. Prevalence of tooth wear in adults. *International Journal of Prosthodontic*, pages 35–42, January 2009.

[34] Y. Jung, J. Lee, Y. Choi, J. Ahn, S. Shin, and J. Huh. A study on the in-vitro wear of the natural tooth structure by opposing zirconia or dental porcelain. *The Journal of Advanced Prosthodontics*, 2(3):111, 2010.

[35] N. Dupriez, A. von Koeckritz, and K. Kunzelmann. A comparative study of sliding wear of nonmetallic dental restorative materials with emphasis on micromechanical wear mechanisms: Wear Mechanisms in Nonmetallic Dental Restorative Materials. *Journal of Biomedical Materials Research Part B: Applied Biomaterials*, 103(4):925–934, May 2015.

[36] M. Etman, M. Woolford, and S. Dunne. Quantitative measurement of tooth and ceramic wear: in vivo study. *International Journal of Prosthodontics*, 21(3):245, 2008.

[37] W. Oh, R. DeLong, and K. Anusavice. Factors affecting enamel and ceramic wear: a literature review. *Journal of Prosthethic Dentistry*, 87(4):451–9, April 2002.

[38] P Magne, MR Pintardo, and R DeLong. Wear of enamel and veneering ceramics after laboratory and chairside finishing procedures. *Journal of Prosthethic Dentistry*, 6(82):669–679, 1999.

[39] A. S. Al-Hiyasat, W. P. Saunders, S. W. Sharkey, G. McR. Smith, and W. H. Gilmour. Investigation of human enamel wear against four dental ceramics and gold. *Journal of Dentistry*, 26(5):487–495, July 1998.

[40] N. Silva, V. Thompson, G. Valverde, P. Coelho, J. Powers, J. Farah, and J. Esquivel-Upshaw. Comparative reliability analyses of zirconium oxide and lithium disilicate restorations in vitro and in vivo. *The Journal of the American Dental Association*, 142, Supplement 2:4S–9S, April 2011.

[41] V. Preis, M. Behr, C. Kolbeck, S. Hahnel, G. Handel, and M. Rosentritt. Wear performance of substructure ceramics and veneering porcelains. *Dental Materials*, 27(8):796–804, August 2011.

[42] J. Nakashima, Y. Taira, and T. Sawase. In vitro wear of four ceramic materials and human enamel on enamel antagonist. *European Journal of Oral Sciences*, 124(3):295–300, June 2016.

[43] 3M ESPE. 3m ESPE TM Lava TM Ultimate CAD/CAM Restorative.

[44] J. Silverman, G. Rosen, and S. Essinger. Applications in Digital Image Processing. *The Mathematics Teacher*, 107(1):46–53, August 2013.

[45] R. DeLong, R. Sakaguchi, W. Douglas, and M. Pintado. The wear of dental amalgam in an artificial mouth: a clinical correlation. *Dental Materials*, 1(6):238–242, 1985.

[46] R. L. Sakaguchi, W. H. Douglas, R. DeLong, and M. R. Pintado. The wear of a posterior composite in an artificial mouth: a clinical correlation. *Dental Materials*, 2(6):235–240, 1986.

APPENDIX

The appendix includes representative tables of raw data obtained from this work.

	Emax	Empress	Celtra	Porcelian	Lava	Glass	Teflon
Contact Angle of Water on Material (°)							
Specimen 1	15.5	39.9	24.398	21.18	64.9	63.12	93.9
Specimen 1	23.3	42.7	22.3	23.5	63.53	72.5	80.69
Specimen 1	22.65	44.9	22.99	22.89	65.12	66.5	
Specimen 2	35.95	57.9	17.9	27.01	73.4		
Specimen 2	39.59	50.08	27.3	25.2	73.53		
Specimen 2	44.9	47.92	18.3	14.6	65.36		
Round 2							
Specimen 1	30.39	54.01	14.83	22.73	58.05	68.8	
Specimen 1	22.08	54.1	17.95	29.51	63.9	62.9	
Specimen 1	24.65	61.61	18.26	29.17	66.35	66.9	
Specimen 2	27.07	60.38	13.38	25.106	63.77		
Specimen 2	26.5	21.95	13.22	31.68	66.88		
Specimen 2	27.92	64.312	21.94	29.06	70.2		
Round 3							
Specimen 1	23.57	46.01	17.97	36.33	63.1	52.19	93.5
Specimen 1	18.94	54.9	16.45	23.9	73.1	55.51	92.9
Specimen 1	21.05	49.1	23.9	28.09	71.18	49.89	84.72
Specimen 2	28.1	41.7	21.9	38.5	58.22		
Specimen 2	22.6	51.6	18.5	51.02	76.05		
Specimen 2	26.3	67.84	24.8	33.5	57.27		
Round 4							
Specimen 1	25.3	40.9	22.44	21.99	61.12	53.03	88.18
Specimen 1	23.25	52.8	17.3	27.7	65.3	57.37	96.85
Specimen 1	24.33	56.58	20.4	28.5	66.2	56.83	99.4
Specimen 2	32.1	62.9	20.5	16.8	72.46		
Specimen 2	23.04	62.43	21	24.76	72.03		
Specimen 2	36.7	68.56	31.97	19.98	67.3		

Figure A.1: This chart presents the contact angle measurements of water on all materials for all trials.

Contact Angle of Biotene on Material (°)							
	Emax	Empress	Celtral	Porcelian	Lava	Glass	Teflon
Specimen 1	28.47	44.29	12.88	14.63	50.88	48.7	44.23
Specimen 1	6.3	24.7	10.78	17.07	50.8	21.67	58.6
Specimen 1	11.11	20.8	8.19	19.97	47.09	24.44	60.8
Specimen 2	18.29	53	12.61	29.8	56.06		
Specimen 2	16.23	32.37	12.68	34.08	55.26		
Specimen 2	16.3	21.13	9.04	24.4	53.77		
Round 2							
Specimen 1	13.97	13.456	4.9	12.3	55.6	48.7	46.9
Specimen 1	13.96	15.27	4.57	15.9	39.47	38.96	57.37
Specimen 1	11.08	9.28	4.81	14.6	33.7	35.17	70.51
Specimen 2	14.83	49.048	6.46	15.6	64.5		
Specimen 2	10.44	36.54	5.14	10.25	34.1		
Specimen 2	10.19	23.98	3.8	8.23	24.3		
Round 3							
Specimen 1	8.72	56.31	15.49	47	58.15	32.5	68.9
Specimen 1	6.5	31.73	17.64	41.322	51.47	44	67.29
Specimen 1	9.18	23.11	19.46	26.99	52.56	41.15	66.6
Specimen 2	13.28	54.77	29.4	18.99	58.1		
Specimen 2	13.9	40.37	19.56	29.8	48.72		
Specimen 2	14.6	35.89	19.79	24.2	52.14		
Round 4							
Specimen 1	25.02	50.26	19.5	41.6	49.15	59.9	63.6
Specimen 1	21.9	45.33	18.45	25.69	47.6	52.3	66.7
Specimen 1	24.3	46.07	18.13	26	43.5	37.63	68.7
Specimen 2	12.5	52.5	16.9	11.79	53.68		
Specimen 2	28.05	51.03	20.2	15.98	42.98		
Specimen 2	24.28	44.17	10.45	18.33	50.57		

Figure A.2: This chart presents the contact angle measurements of Biotene on all materials for all trials.

Speciemen	MATLAB Angle(°)	Goniometer Angle (°)	Percent Error (%)
Biotene on Celtra	14.57	15.49	5.94
Biotene on Celtra	21.02	19.79	-6.22
Biotene on Emax	27.45	29.11	5.70
Biotene on Emax	48.59	43.6	-11.44
Biotene on Empress	56.8	56.3	-0.89
Biotene on Empress	44.6	43.38	-2.81
Biotene on Porcelian	14.16	14.83	4.52
Biotene on Glass	31.12	32.19	3.32
Biotene on Glass	50.98	54.2	5.94
Biotene on Lava	54.16	57.97	6.57
Biotene on Lava	58.56	58.06	-0.86
Biotene on PTFE	70.11	71.84	2.41
Biotene on PTFE	62.76	69.2	9.31
Water on Celtra	20.79	19.53	-6.45
Water on Celtra	21.4	21.26	-0.66
Water on Emax	24.25	21.94	-10.53
Water on Emax	65.4	37.37	-75.01
Water on Empress	64.5	72.02	10.44
Water on Empress	47.39	45.07	-5.15
Water on Porcelian	27.5	22.6	-21.68
Water on Porcelian	30.35	32.82	7.53
Water on Glass	65.13	67.34	3.28
Water on Glass	63.75	63.38	-0.58
Water on Lava	58.5	73.8	20.73
Water on Lava	59.1	59.41	0.52
Water on PTFE	67.83	68.15	0.47
Water on PTFE	71.04	73.94	3.92

Figure A.3: The chart above shows the contact angle measurements obtained the goniometer for select trials and compares it the angle measurements obtained from MATLAB. For each specimen, a percent error is evaluated to determine the error between the goniometer and MATLAB results.